

## Coherent Magnetization Precession in Ferromagnetic (Ga,Mn)As Induced by Picosecond Acoustic Pulses

A. V. Scherbakov,<sup>1</sup> A. S. Salasyuk,<sup>1,2</sup> A. V. Akimov,<sup>1,3</sup> X. Liu,<sup>4</sup> M. Bombeck,<sup>2</sup> C. Brüggenmann,<sup>2</sup> D. R. Yakovlev,<sup>1,2</sup> V. F. Sapega,<sup>1</sup> J. K. Furdyna,<sup>4</sup> and M. Bayer<sup>1,2</sup>

<sup>1</sup>*Ioffe Physical-Technical Institute of the Russian Academy of Sciences, 194021 St. Petersburg, Russia*

<sup>2</sup>*Experimentelle Physik 2, Technische Universität Dortmund, D-44227 Dortmund, Germany*

<sup>3</sup>*School of Physics and Astronomy, University of Nottingham, Nottingham NG7 2RD, United Kingdom*

<sup>4</sup>*Department of Physics, University of Notre Dame, Notre Dame, Indiana 46556, USA*

(Received 26 April 2010; published 9 September 2010)

We show that the magnetization of a thin ferromagnetic (Ga,Mn)As layer can be modulated by picosecond acoustic pulses. In this approach a picosecond strain pulse injected into the structure induces a tilt of the magnetization vector  $\mathbf{M}$ , followed by the precession of  $\mathbf{M}$  around its equilibrium orientation. This effect can be understood in terms of changes in magnetocrystalline anisotropy induced by the pulse. A model where only one anisotropy constant is affected by the strain pulse provides a good description of the observed time-dependent response.

DOI: 10.1103/PhysRevLett.105.117204

PACS numbers: 75.78.Jp, 43.35.+d, 75.30.Gw, 75.50.Pp

The success of semiconductors in today's modern technology arises from our ability to tailor their electrical and optical properties on a detailed level. High crystal quality of semiconductors allows one to implement tools for fast manipulation of properties, which is of interest both for fundamental studies and for applications. In this respect, manipulation by high-frequency ( $10^9$ – $10^{12}$  Hz) acoustic waves has become increasingly attractive for extending traditional acousto-electronics and acousto-optics to gigahertz (GHz) and terahertz (THz) frequency ranges [1]. During the last decade intense efforts have been undertaken to extend the application spectrum by making semiconductors also magnetic. Therefore one might also seek for ultrafast control of semiconductor magnetism by high-frequency sound. Access to such control could be obtained through the strong sensitivity of the magneto-crystalline anisotropy (MCA) in ferromagnetic semiconductors, such as (Ga,Mn)As to strain [2–4].

Several methods to control MCA in (Ga,Mn)As films by applying an electric field and varying doping have already been developed [5–9]. In ultrafast experiments, modulation of MCA was realized by optically induced increases of carrier density and lattice temperature [10–12]; as well as femtosecond switching of magnetization [13] was demonstrated. The application of ultrafast optical methods, however, is limited by effects such as simultaneous generation of large numbers of nonequilibrium carriers and phonons. The control of MCA by acoustic waves would allow ultrafast manipulations of magnetization in a ferromagnetic semiconductor without these side effects.

The goal of the present work is to inject an ultrashort high-amplitude acoustic wave packet into a ferromagnetic (Ga,Mn)As layer, and to monitor the relevant magnetization changes. We use the methods of ultrafast acoustics, which enable the generation of picosecond strain pulses in

solids [14]. Strain pulses with the amplitude up to  $10^{-3}$  generated by femtosecond optical pulses in thin metal films and injected into crystalline substrates (e.g., GaAs) have been shown to travel over millimeter distances at low temperatures, and up to  $100\ \mu\text{m}$  at room temperature [15]. Such a strain pulse has a direct, short and intense impact on the MCA of the layer, and thus can act as an instrument for magnetization control.

In this Letter we show that strain pulses injected into a ferromagnetic (Ga,Mn)As layer induce a tilt of magnetization from its stationary equilibrium orientation, followed by coherent precession of the magnetization at a frequency of  $\sim 10$  GHz. This process can be well described by a simple model where the strain pulse induces a change in the MCA of (Ga,Mn)As.

The sample used in our studies consists of a single  $\text{Ga}_{0.95}\text{Mn}_{0.05}\text{As}$  layer with a thickness  $d = 200$  nm grown by low-temperature molecular beam epitaxy on a semi-insulating (001) GaAs substrate. SQUID magnetometry shows that the Curie temperature of the sample is 60 K and the saturation magnetization  $M$  is  $20\ \text{emu}/\text{cm}^3$ . The magnetic layer is under an in-plane compressive strain that leads to an in-plane orientation of easy magnetization axis [3]. The values of the internal strain components obtained from x-ray diffraction are  $-2 \times 10^{-3}$  for the in-plane compressive strain, and  $1.9 \times 10^{-3}$  for the out-of-plane tensile strain. In the absence of an external magnetic field the spontaneous magnetization  $\mathbf{M}$  of magnetic domains lies in the layer plane at low temperatures. The magnetic field  $\mathbf{B}$  applied along the  $z$  axis (i.e., perpendicular to the layer) turns  $\mathbf{M}$  out of the layer plane, as shown in Fig. 1(a). We will describe the direction of  $\mathbf{M}$  in a single magnetic domain by the angles  $\theta$  and  $\psi$  as defined in Fig. 1(a).

Our experiments were carried out at  $T = 1.6$  K in a cryostat equipped with a superconducting magnet. The

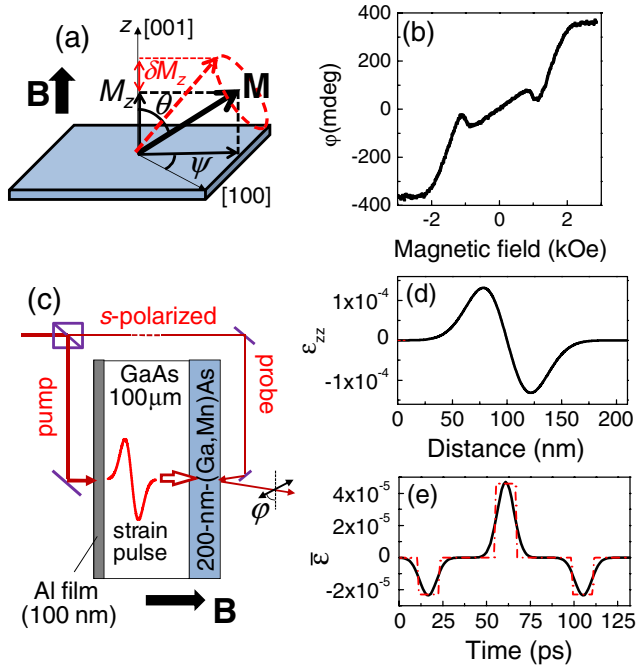


FIG. 1 (color online). (a) Schematic of sample and magnetic field orientations. The precession of  $\mathbf{M}$  around its equilibrium direction results in a modulation of  $M_z$ . (b) Magnetic field dependence of the KR angle measured in the absence of strain pulses. (c) Schematic of pump-probe experiments with strain pulses. The laser characteristics are wavelength 800 nm, pulse duration 200-fs, repetition rate 100 kHz; pump and probe spot diameters are 300 and 150- $\mu\text{m}$  respectively; the energy density per pulse are 2 mJ/cm<sup>2</sup> (pump) and 10  $\mu\text{J}/\text{cm}^2$  (probe). (d) Spatial shape of strain pulse  $\varepsilon_{zz}$  injected into the GaAs substrate. (e) Time evolution of relative thickness of the (Ga,Mn)As layer  $\bar{\varepsilon}(t)$ .

projection of  $\mathbf{M}$  on the  $z$  axis,  $M_z = M \cos\theta$ , is measured by monitoring the Kerr rotation (KR), i.e., the angle  $\varphi$  between the linear polarizations of the light incident on and reflected from the (Ga,Mn)As layer, given by

$$\varphi = \arctan\left(\text{Re}\left[i\frac{r^+ - r^-}{r^+ + r^-}\right]\right), \quad (1)$$

where  $r^+$  and  $r^-$  are complex reflection coefficients for left- and right-handed circularly polarized light. In general, a difference between  $r^+$  and  $r^-$  may arise from several causes. In (Ga,Mn)As layers KR has a contribution from the magneto-optical Kerr effect [16] and in our experimental geometry the KR angle  $\varphi$  is proportional to the  $\mathbf{M}$  component along the  $z$  axis,  $M_z$ , i.e.,  $\varphi \propto M_z$ .

Figure 1(b) shows the magnetic field dependence of the angle  $\varphi$  at stationary equilibrium conditions. The measured field dependence of this quantity is typical for (Ga,Mn)As layers with the easy magnetization axis in the (001) plane [17]. Note that the value of  $\varphi$ —and thus of  $M_z$ —increases with  $B$  and finally saturates at  $B > 2$  kOe, i.e., when  $\mathbf{M} \parallel \mathbf{B}$  and  $M_z = M$ . The dip or kick observed around  $B = 1$  kOe is known to be caused by optical

interference effects [17]. The field dependence of the magnetization can be analyzed by minimizing the free energy with respect to  $\theta$ , as described in Ref. [18], allowing us to obtain the anisotropy parameters  $H_{2\perp}$ ,  $H_{4\perp}$ ,  $H_{2\parallel}$ , and  $H_{4\parallel}$  of the sample, i.e., the perpendicular uniaxial, perpendicular cubic, in-plane uniaxial, and in-plane cubic anisotropy fields, respectively. The following values of anisotropy fields provide the best fit of the experimental curve:  $(4\pi M + H_{2\perp}) = 1.82$  kOe,  $H_{4\perp} = 0.66$  kOe,  $H_{2\parallel} = 0$ , and  $H_{4\parallel} = 1.97$  kOe. These values are typical for ferromagnetic (Ga,Mn)As layers with Mn content of ca. 5% and with in-plane easy magnetization axes along [100] or [010] directions [18].

In the ultrafast acoustic experiments [Fig. 1(c)] we generate strain pulses, which modify the MCA, thus, causing the magnetization to turn from its equilibrium position, and monitor in real time the resulting changes in  $M_z$ . Picosecond strain pulses are generated in a 100-nm thick Al film deposited on the back side of the GaAs substrate. The film is excited by optical pump pulses from an amplified femtosecond laser. The calculated [19] spatial shape of the strain pulse  $\varepsilon_{zz}(z, t)$  injected into the substrate is shown in Fig. 1(d). The pulse propagates in GaAs with a longitudinal sound velocity  $\nu = 4.8$  km/s, and in time  $t_0 = l_0/\nu \approx 22$  ns (where  $l_0 = 105$   $\mu\text{m}$  is the substrate thickness) reaches the magnetic layer. At the open surface of the film the strain pulse is reflected with a phase inversion, and travels back towards the GaAs substrate. Thus the thickness  $d$  of the (Ga,Mn)As layer is modulated by the strain pulse. The temporal profile of the relative layer thickness modulation can be written as

$$\bar{\varepsilon}(t) = \frac{\Delta d(t)}{d} = \frac{1}{d} \int_0^d \varepsilon_{zz}(t, z) dz, \quad (2)$$

where  $\Delta d(t)$  is the time evolution of the film thickness change, and  $z = 0$  corresponds to the interface between the GaAs substrate and (Ga,Mn)As film. The time evolution of  $\bar{\varepsilon}(t)$  for our experimental conditions is shown in Fig. 1(e) by the solid line. It is seen that the strain pulse results in compressive and tensile perturbations of the film, separated by intervals when  $\Delta d = 0$ .

The time evolution of the magnetization is monitored by probing  $M_z$  with subpicosecond time resolution. We measure the strain-induced modulation of the KR angle  $\varphi$  as a function of the time delay  $t$  between pump and probe pulses. The optical probe pulse, split from the same laser beam, is focused to the spot on the (Ga,Mn)As layer opposite to the pump excitation [Fig. 1(c)]. Figure 2(a) shows the time evolution of the KR angle change  $\Delta\varphi(t)$  measured at different  $B$ , where  $t = 0$  corresponds to the time when the strain pulse reaches the (Ga,Mn)As layer. In the time interval from  $t = 0$  to  $t = 125$  ps indicated in Fig. 2(a) by the vertical arrow the strain pulse travels through the (Ga,Mn)As layer to the edge of the sample and back to the GaAs substrate, so that for  $t > 125$  ps the acoustic wave packet is no more present in the (Ga,Mn)As layer. The remarkable experimental result is that in the

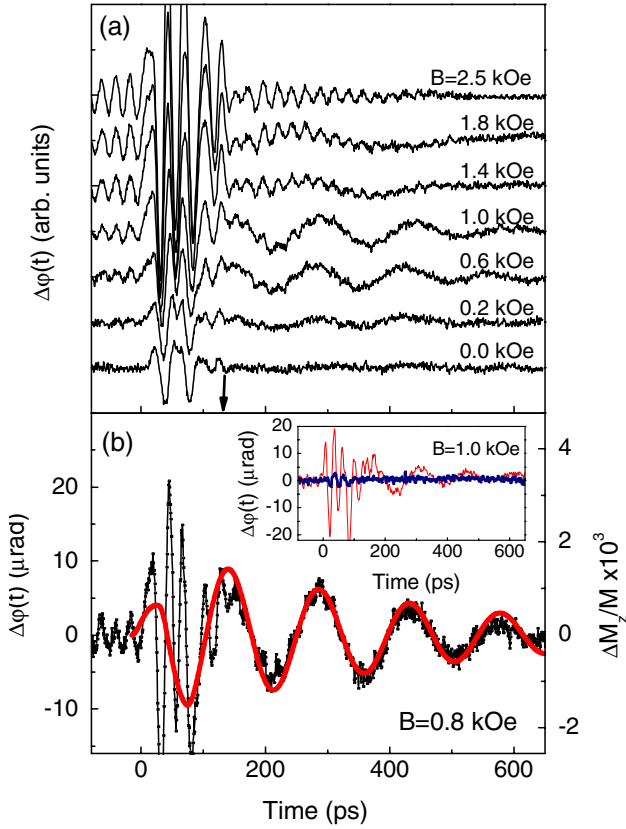


FIG. 2 (color online). Strain pulse-induced KR angle changes  $\Delta\varphi(t)$  measured at various magnetic fields (a) and at  $B = 0.8$  kOe (b). The value  $t = 0$  corresponds to the time when the strain pulse enters the (Ga,Mn)As layer, and the vertical arrow shown in panel (a) indicates the time when the strain pulse leaves the (Ga,Mn)As layer. The thick solid curve in (b) is  $\Delta M_z(t)/M$  calculated for  $d\theta/d\varepsilon_{zz} = 60$  rad,  $F = 6.86$  GHz and for a precession decay time of 400 ps. Inset in (b):  $\Delta\varphi(t)$  when the pump excitation is opposite to the probe spot (thin red line) and when they are displaced by  $100 \mu\text{m}$  (thick blue line); the diameters of pump and probe spots are 100 and  $50 \mu\text{m}$ , respectively.

field range  $0 < B < 2$  kOe and at  $t > 150$  ps, i.e., after the strain pulse itself has already left the ferromagnetic layer, the KR signal shows pronounced oscillations with a frequency  $\sim 10$  GHz. These low-frequency oscillations are not detected at  $B = 0$ . They only appear when  $B$  is applied; and they disappear at high magnetic fields above 2.5 kOe. These oscillations last for times  $\sim 1$  ns and their frequency and amplitude depend on  $B$ . As an example, the KR signal obtained at  $B = 0.8$  kOe, where the low-frequency oscillations have the highest amplitude, is shown in Fig. 2(b).

In addition to these low-frequency oscillations,  $\Delta\varphi(t)$  also reveals more complex fast oscillating features. Specifically, high-frequency oscillations of about 44 GHz are observed at  $B > 1$  kOe in a wide time interval. Oscillations of this type have been seen earlier in GaAs [20], and are ascribed to interference of the probe beams reflected from the sample surface and from the strain wave packet propagating in the sample. Magnetic field makes

these oscillations evident in the KR due to the circular dichroism of the paramagnetic GaAs substrate when the strain pulse propagates through it at  $t < 0$  and  $t > 125$  ps [see Eq. (1)]. There is also a pronounced fast oscillating contribution to  $\Delta\varphi(t)$  in the time interval  $0 < t < 125$  ps, i.e., when the strain pulse is traveling in the (Ga,Mn)As layer. This high-frequency contribution is present at all fields, including  $B = 0$ . Apparently this contribution is due to the anisotropy of the elasto-optical constants in the strained (Ga,Mn)As layer. We also do not exclude the modification of elastic properties due to interaction of phonons with the magnetic excitation. A detailed analysis of this observation should be performed in terms of the theoretical approach presented in Ref. [21], but this is beyond the scope of the present work.

All contributions, including slow oscillations, are induced by the strain pulse, and we safely can exclude the effect of the heat pulse generated in the metal film together with the strain pulses. The heat pulse is the flux of incoherent ballistic phonons which follow the strain pulse with a delay  $\sim 100$  ps, and has duration longer than 200 ps depending on the excitation power [22]. Thus, the heat pulse cannot induce the coherent signals shown in Fig. 2. The abrupt decrease of the signal [see inset in Fig. 2(b)], when the pump and the probe excitation are not opposite to each other, supports the statement that LA heat pulses are insignificant in the described experiments [23].

In what follows we will concentrate on the long-lived low-frequency oscillations of  $\Delta\varphi(t)$ , which we attribute to the modulation of  $M_z$  in (Ga,Mn)As. We consider these oscillations to be due to the strain-induced tilt of the magnetization vector  $\mathbf{M}$ , followed by a coherent precession of  $\mathbf{M}$  around its equilibrium direction. The frequency of these oscillations is in the GHz range typical for such precession, as established by ferromagnetic resonance experiments [24]. The amplitude of the oscillations is expected to be negligible at  $B = 0$ , where the net  $z$  component of  $\mathbf{M}$  vanishes. At high fields,  $B > 2$  kOe,  $\mathbf{M}$  is practically parallel to  $\mathbf{B}$  ( $\theta \rightarrow 0$ ), and the temporal modulation of  $M_z$  also becomes negligibly small. Thus, the strain-induced tilt of the magnetization and its precession should be most conspicuous in the range of magnetic field where the direction of  $\mathbf{M}$  is determined by the balance between the external magnetic field and the MCA field. All these arguments can be applied to the behavior of  $\Delta\varphi(t)$  observed experimentally in the range  $0 < B < 2$  kOe.

We now analyze the magnetization kinetics associated with the strain pulse propagating in the (Ga,Mn)As layer. In the presence of a magnetic field applied normal to the layer, a (Ga,Mn)As film with a thickness of 200 nm has a single value of  $M_z$ , in that respect behaving like a single domain [25]. We may, therefore, express quantitatively the temporal evolution of magnetic anisotropy in the (Ga,Mn)As layer through the relative change of the layer thickness  $\bar{\varepsilon}(t)$  given by Eq. (2). Since then any modification of the built-in stationary strain produced by  $\bar{\varepsilon}(t)$  will tilt the equilibrium magnetization by an angle  $\Delta\theta_\varepsilon(t)$

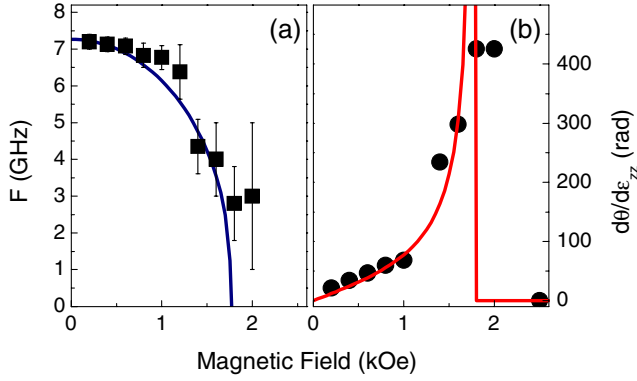


FIG. 3 (color online). Magnetic field dependencies of the precession frequency  $F$  (a) and the angle variation parameter  $d\theta/d\varepsilon_{zz}$  (b). Solid lines are the calculated dependences of  $F$  and  $d\theta/d\varepsilon_{zz}$  obtained for  $dH_{2\perp}/d\varepsilon_{zz} = 850$  kOe.

relative to its unperturbed stationary direction. When  $\bar{\varepsilon}(t)$  is much less than the built-in equilibrium strain,  $\Delta\theta_\varepsilon(t)$  is proportional to  $\bar{\varepsilon}(t)$  and we may write

$$\Delta\theta_\varepsilon(t) = \frac{d\theta}{d\varepsilon_{zz}} \bar{\varepsilon}(t) = \frac{d\theta}{dH_{2\perp}} \frac{dH_{2\perp}}{d\varepsilon_{zz}} \bar{\varepsilon}(t). \quad (3)$$

In Eq. (3) we have assumed that  $\bar{\varepsilon}(t)$  changes only the value of the uniaxial perpendicular term  $H_{2\perp}$  of magnetocrystalline anisotropy, and the magnetization is tilted only by the change in the angle  $\theta$  [26].

To simplify the analysis, we approximate  $\bar{\varepsilon}(t)$  by square pulses shown in Fig. 1(e) by dash-dot lines. Then in the time intervals when  $\bar{\varepsilon}(t)$  remains constant  $\mathbf{M}(t)$  possesses a circular precession with frequency  $F$  around the direction defined by  $\theta$  and  $\Delta\theta_\varepsilon(t)$ . Every time when  $\bar{\varepsilon}(t)$  changes to another constant value,  $\mathbf{M}(t)$  starts to precess circularly around another, corresponding to  $\bar{\varepsilon}(t)$ , direction. With this simplification we seek the values of  $d\theta/d\varepsilon_{zz}$  and the precession frequency  $F$  that give the best agreement between the calculated temporal evolution of  $\Delta M_z/M$  and the detected KR signal  $\Delta\varphi(t)$  at a given field. An example of the fit  $\Delta M_z(t)/M$  for  $d\theta/d\varepsilon_{zz} = 60$  radian and  $F = 6.86$  GHz, which fits well the experimental signal for  $B = 0.8$  kOe is shown by the solid line in Fig. 2(b). A similar procedure was used for other values of  $B$ , yielding the corresponding magnetic field dependences of  $d\theta/d\varepsilon_{zz}$  and  $F$ , which are shown by symbols in Fig. 3. The solid curve in Fig. 3(a) shows the magnetic field dependence of the frequency  $F$  calculated using the MAC parameters for our sample (for details see Ref. [18]). The experimental and calculated dependences demonstrate a clear decrease of  $F$  with increasing  $B$ , and agree well with each other. The solid curve in Fig. 3(b) is the calculated dependence of  $d\theta/d\varepsilon_{zz}$  obtained by minimizing the free energy with respect to  $\theta$ , assuming a field-independent value of  $dH_{2\perp}/d\varepsilon_{zz}$  as a fitting parameter [see Eq. (3)]. Excellent

agreement with experimental data is achieved using  $dH_{2\perp}/d\varepsilon_{zz} = 850$  kOe. This value is in good agreement with the data recently reported for several (Ga,Mn)As samples [3].

To conclude, we have demonstrated the effect of high-frequency acoustic pulses on the magnetization of a ferromagnetic (Ga,Mn)As layer. Based on the experimental results, we suggest that control of magnetization by sub-THz acoustic pulses may be realized.

The authors thank L. E. Golub, N. S. Averkiev, and S. A. Tarasenko for valuable discussions. This work was supported by the Deutsche Forschungsgemeinschaft via Koselleck Programme (Grant No. BA1549/14-1), the European Community's Seventh Framework Programme under Grant Agreement No. 214954 (HERODOT), the Russian Foundation for Basic Research, the Russian Academy of Sciences, CRDF (Grant RUP 1-2890-ST-07), and the National Science Foundation (Grants DMR06-03752 and DMR10-05851).

- 
- [1] M.R. Armstrong *et al.*, *Nature Phys.* **5**, 285 (2009).
  - [2] J. Zemen *et al.*, *Phys. Rev. B* **80**, 155203 (2009).
  - [3] M. Glunk *et al.*, *Phys. Rev. B* **79**, 195206 (2009).
  - [4] U. Welp *et al.*, *Phys. Rev. Lett.* **90**, 167206 (2003).
  - [5] M. Overby *et al.*, *Appl. Phys. Lett.* **92**, 192501 (2008).
  - [6] A. W. Rushforth *et al.*, *Phys. Rev. B* **78**, 085314 (2008).
  - [7] C. Bihler *et al.*, *Phys. Rev. B* **78**, 045203 (2008).
  - [8] Sunjae Chung *et al.*, *Solid State Commun.* **149**, 1739 (2009).
  - [9] D. Chiba *et al.*, *Nature (London)* **455**, 515 (2008).
  - [10] J. Qi *et al.*, *Appl. Phys. Lett.* **91**, 112506 (2007).
  - [11] Y. Hashimoto, S. Kobayashi, and H. Munekata, *Phys. Rev. Lett.* **100**, 067202 (2008).
  - [12] E. Rozkotová *et al.*, *Appl. Phys. Lett.* **92**, 122507 (2008).
  - [13] G. V. Astakhov *et al.*, *Appl. Phys. Lett.* **86**, 152506 (2005).
  - [14] [http://en.wikipedia.org/wiki/Picosecond\\_ultrasonics](http://en.wikipedia.org/wiki/Picosecond_ultrasonics).
  - [15] H.-Y. Hao and H.J. Maris, *Phys. Rev. B* **63**, 224301 (2001).
  - [16] R. Lang *et al.*, *Phys. Rev. B* **72**, 024430 (2005).
  - [17] G. P. Moore *et al.*, *J. Appl. Phys.* **94**, 4530 (2003).
  - [18] X. Liu *et al.*, *J. Appl. Phys.* **98**, 063904 (2005).
  - [19] G. Tas and H.J. Maris, *Phys. Rev. B* **49**, 15046 (1994).
  - [20] O.B. Wright *et al.*, *Phys. Rev. B* **64**, 081202 (2001).
  - [21] O. Matsuda *et al.* *Phys. Rev. B* **77**, 224110 (2008).
  - [22] B. Perrin, E. Péronne, and L. Belliar, *Ultrasonics* **44**, e1277 (2006).
  - [23] N.M. Stanton and A. J. Kent, *Phys. Rev. B* **73**, 220301(R) (2006).
  - [24] X. Liu, Y. Sasaki, and J.K. Furdyna, *Phys. Rev. B* **67**, 205204 (2003).
  - [25] T. Shono *et al.*, *Appl. Phys. Lett.* **77**, 1363 (2000).
  - [26] Actually, if  $\bar{\varepsilon}(t)$  also has an effect on the angle  $\psi$ , the in-plane multidomain structure of (Ga, Mn)As should average out this effect.